Journal of Petroleum Exploration and Production Technology (2023) 13:813–826
https://doi.org/10.1007/s13202-022-01569-z

ORIGINAL PAPER - PRODUCTION GEOLOGY

# Experimental measurements of $CO_2$ adsorption on Indonesian low-rank coals under various conditions

**Theodora Noely Tambaria[1,2] · Yuichi Sugai[1] · Ferian Anggara[2,3]**

Received: 21 June 2022 / Accepted: 11 September 2022 / Published online: 29 September 2022


## Abstract

In this study, the $CO_2$ adsorption capacity was measured on Indonesian low-rank coals in the raw and dry conditions in powder and block states using different coal sample preparation to estimate $CO_2$ sequestration and storage potential. Coal sample specimens were taken from three different areas in the South Sumatra Basin, Indonesia. The adsorption experiments were performed using the volumetric method at a temperature of 318.15 K and pressure up to 3 MPa. The $CO_2$ excess adsorption capacity of powder coal is always higher than block coal. Moreover, decreasing moisture content by the drying process increases $CO_2$ adsorption capacity on coal. Based on fitted $CO_2$ adsorption experimental data with the Langmuir and Freundlich isotherm model, the adsorption occurs on monolayer and multilayer at various conditions. Langmuir volume capacity and pressure show drying and crushing process increased adsorption capacity. However, the drying process affects more the capability of coal to adsorb $CO_2$ than the powdered sample, especially in low-rank coal. It was also observed adsorption capacity is directly proportional to huminite content in the coal. Due to lower moisture and higher huminite contents, the dried WB coal powder had the highest $CO_2$ adsorption capacity over the other coal samples in similar sample conditions. Altogether, this study may provide a better understanding in $CO_2$ adsorption on low-rank coal with different coal sample preparation resulting in different $CO_2$ adsorption capacity.

**Keywords** $CO_2$ sequestration · $CO_2$ adsorption capacity · Low-rank coal · Different sample conditions · Adsorption factor

## List of symbols

| | |
|---|---|
| $R_0$ | Huminite reflectance (%) |
| $VM_{daf}$ | Volatile matter (dry ash-free basis) (%) |
| $V_{rc}$ | Reference cell volume ($cm^3$) |
| $V_{sc}$ | Sample cell volume ($cm^3$) |
| $V_{void}$ | Void volume ($cm^3$) |
| $n^{ex}$ | Gibbs excess adsorption (mmol $g^{-1}$) |
| $R$ | Molar gas constant (8.314 J $mol^{-1}$ $K^{-1}$) |
| $T$ | Temperature (K) |
| $m$ | Mass of coal (g) |
| $P_{rc}$ | Pressure at reference cells (MPa) |
| $P_{sc}$ | Pressure at sample cells (MPa) |
| Subscripted $i$ | Initial condition |
| Subscripted $f$ | Final condition |
| $Z$ | Compressibility factor |
| $\omega$ | Acentric factor of gas |
| $P_r$ | Reduced pressure |
| $T_r$ | Reduced temperature |
| $P_c$ | Critical pressure |
| $T_c$ | Critical temperature |
| $G_a$ | Langmuir isotherm model adsorbed-gas storage capacity |
| $V_L$ | Langmuir volume |
| $P_L$ | Langmuir pressure |
| $Q_e$ | Freundlich isotherm model adsorbed-gas storage capacity |
| $K_f$ | The constant of Freundlich isotherm model |
| $n$ | Heterogeneity factor |

✉ Theodora Noely Tambaria
theodora.noely.t@mail.ugm.ac.id

[1] Department of Earth Resources Engineering, Kyushu University, 744, Motooka, Nishiku, Fukuoka 819-0395, Japan

[2] Department of Geological Engineering, Faculty of Engineering, Universitas Gadjah Mada, Jalan Grafika No. 2 Kampus UGM Bulaksumur, D.I. Yogyakarta 55281, Indonesia

[3] Unconventional Geo-Resources Research Group, Faculty of Engineering, Universitas Gadjah Mada, Jalan Grafika No. 2 Kampus UGM Bulaksumur, D.I. Yogyakarta 55281, Indonesia

## Introduction

The storage of $CO_2$ is one of the alternatives to reduce $CO_2$ emissions to the atmosphere. Geological storage of $CO_2$ is one of the best methods due to the large storage capacity over a long period. Previous study has shown that geological storage can contain huge volumes of $CO_2$ while also adding benefits such as reduced negative impact and enhanced oil recovery (EOR) (Vo Thanh et al. 2019; AlRassas et al. 2021; Khanal and Shahriar 2022; Safaei-Farouji et al. 2022). Geological sequestration in coal seams allows the storing of $CO_2$ since $CO_2$ will bind to the coal, causing the $CO_2$ to be trapped physically in the coal (Wahid et al. 2018). Adsorption is the primary mechanism for $CO_2$ storage in coal seams, accounting for approximately 95–98% of total storage (De Silva et al. 2012). Moreover, $CO_2$ urges $CH_4$ to escape from the coal seam and allows for enhanced coal bed methane (ECBM) which may minimize the cost of sequestration (Day et al. 2010; Anggara et al. 2014, 2016).

Low-rank coal can adsorb $CO_2$ in higher volume than high-rank coal (Kolak and Burruss 2004; Sripada et al. 2018), but low-rank coal has the most significant water adsorption capacity compared to the other coal rank (Liu et al. 2018). Changes in moisture content have become an exciting topic in the field of identifying the possibility of increasing the storage of $CO_2$ in the coal seam (Hao et al. 2018; Gao et al. 2019; Abunowara et al. 2020). The comparisons between dry and wet coal have been analyzed in many studies to identify the moisture effect on $CO_2$ storage capacity (Pan et al. 2010; Švábová et al. 2012; Chen et al. 2018).

Coal powder samples have been mainly used to analyze the influence of moisture on the $CO_2$ adsorption (Gensterblum et al. 2013; Abunowara et al. 2020). Powdering process has affects porous structure, especially in low-rank coal (Mangi et al. 2022). Using coal powder samples for the adsorption experiments requires additional analysis since physical changes cause differences in the amount of gas adsorbed. The varying sizes of coal particles result in different gas adsorption capacities (Anggara et al. 2010). Nevertheless, one of the main problems with using coal powder is that it hardly represents the in situ underground storage conditions that occur in a compact form. To address this issue, one of the ways is to compare gas adsorption on coal powder and compact coal samples. A study has shown different adsorption capacities on coal powder and coal lumps due to different surface areas (Kim et al. 2019).

Various experimental adsorption methods are not only based on coal samples' conditions but also on pressure and temperature setups. Coal injected with $CO_2$ injected into coal under high pressure was a commonly used setup since it increases the $CH_4$ recovery and $CO_2$ storage rates (Busch et al. 2003b; Zhu et al. 2019). However, injecting $CO_2$ under high pressure resulted in problems such as reduced coal permeability (Wang et al. 2016) and the possibility of over-caprock integrity and leakage (Masum et al. 2022). Temperature is also a critical factor in adsorption since higher temperature will increase the kinetic energy of the gas molecules resulting in lower adsorption capacity (Zhou et al. 2019). Furthermore, the effect of $CO_2$ injection above 4 MPa at 323.15 K on the cumulative desorption of $CH_4$ gas is weakened (Wen et al. 2022).

Isotherm adsorption model is used on experimental data to identify how $CO_2$ adsorbed on coal. Langmuir and Freundlich are two adsorption isotherms parameters that are widely used to analyze adsorption capacity (Kalam et al. 2021). Even though Langmuir and Freundlich are commonly used, the results will vary depending on the adsorbents and gas injected (Guarín Romero et al. 2018; Hao et al. 2021). The adsorption characteristics are correlated with various coal compositions (Laxminarayana and Crosdale 1999; Dutta et al. 2011; Anggara et al. 2014, 2016). Thus far, none of these papers have successfully obtained isotherm parameters using various coal sample conditions.

Coal from South Sumatra Basin has various moisture contents (Sosrowidjojo 2013) and consists of mainly low-rank coal (Amijaya and Littke 2005). South Sumatra coal basin is recognized as one of Indonesia's largest and most important coal mining regions (Amijaya and Littke 2005; Belkin et al. 2009). Coal from this area has CBM potential resources about up to 40% out of total potential resources in Indonesia (Wahid et al. 2018). The evolution of research from CBM to the possibility of ECBM recovery improves ECBM study in the South Sumatera Basin. Coal samples from two coal seams in the South Sumatera Basin were taken and proven to have the potentials of $CO_2$ geological storage and ECBM recovery (Anggara et al. 2010; Anggara 2017). Numerical simulation has also been done on South Sumatera CBM field to discover a possibility of ECBM recovery (Wahid et al. 2018). Furthermore, South Sumatera coal exhibits the heterogeneous coal characteristics, which affect $CO_2$ adsorption on coal (Afikah et al. 2018). Most of these studies have concentrated only on some coal samples representing adsorption characteristics from an area. Meanwhile, different coal seams have different surface areas (Karayiğit et al. 2018) and pore parameters (Wu et al. 2014). The differences would lead to a variety of gas adsorption capabilities. Increasing accuracy is a meaningful value for predictive $CO_2$ adsorption on South Sumatera.

This study aims to comprehensively investigate coal characteristics and sample preparation for $CO_2$ adsorption capacity and analyze isotherm parameters. In contrast with another study, a coal sample was taken from the same

coal seam in a different area to highlight the differences in similarity of organic matter for adsorbing $CO_2$. Even though this study used samples with various conditions, $CO_2$ adsorption was done with low-medium pressure at 318.15 K to consider the possibility of $CO_2$ storage and ECBM. The volumetric method was used to support $CO_2$ adsorption in various forms and water conditions (Battistutta et al. 2012; Kim et al. 2019), even though equipment's ability of the volumetric method to detect up to high is not used to the fullest. The progress to identifying $CO_2$ adsorption capacity on coal was detailed in Fig. 1. Firstly, three coal samples were taken from the thickest coal seam in the South Sumatera basin (seam B) from a different area (Fig. 2). Then samples were prepared onto coal powder and coal block in dry and raw coal conditions. $CO_2$ was injected with the volumetric method on 318.15 K and a maximum pressure of 3 MPa. Langmuir and Freundlich's isotherm model were used to obtain the isotherm parameter for the study area. Finally, coal characteristics and organic matter are used to evaluate the $CO_2$ adsorption properties of coal.

## Sample preparation

### Coal characteristic measurements

Samples were taken from South Sumatra Basin, Indonesia, and coal seams were selected from the thickest coal seams in three areas, namely West Banko (WB), East Banko (EB), and North Muara Tiga Besar (NMTB). Coal samples slightly differ in coal lithotype where coal samples from WB were banded-dull, coal samples from EB were dull, and coal samples from North Muara Tiga Besar NMTB were banded-dull (Fig. 3). The coal characteristics were performed based on the proximate and petrography analysis. The moisture content of coal powder was determined based on the ASTM D3173-73 guidelines by

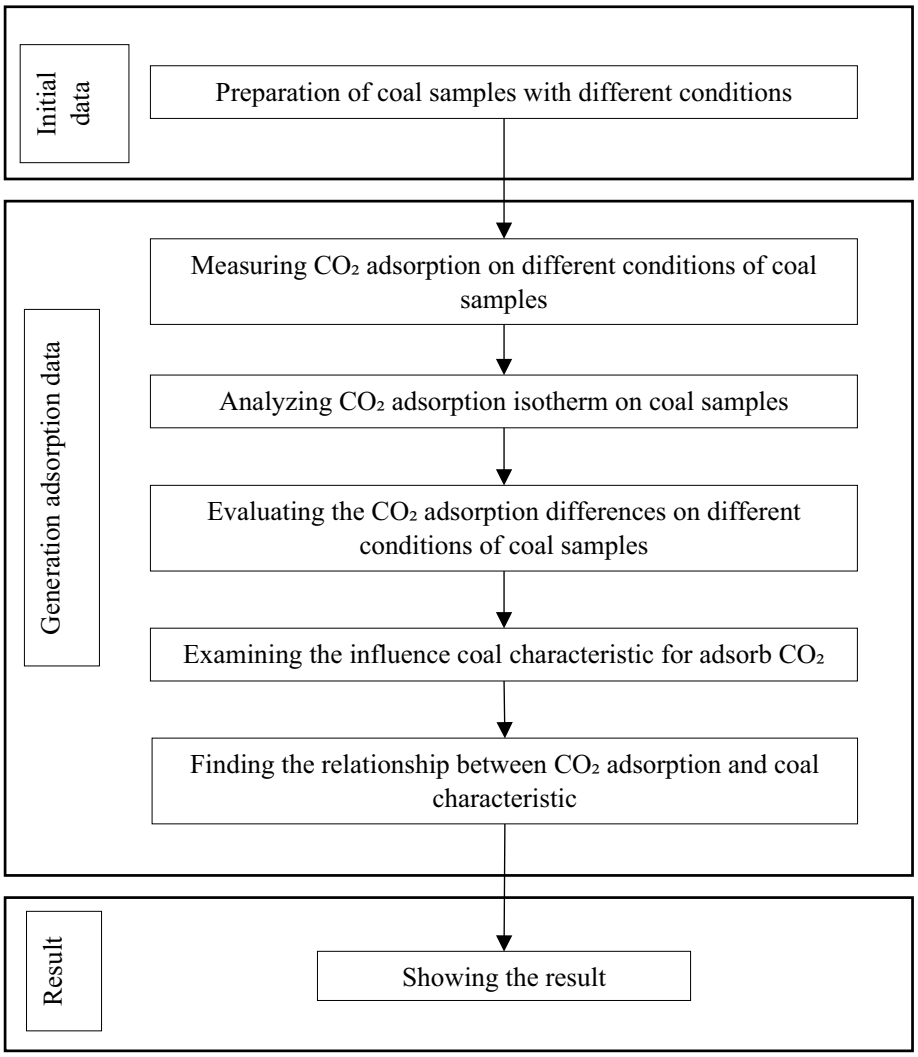


**Fig. 1** General sketch of $CO_2$ adsorption on coal with various conditions

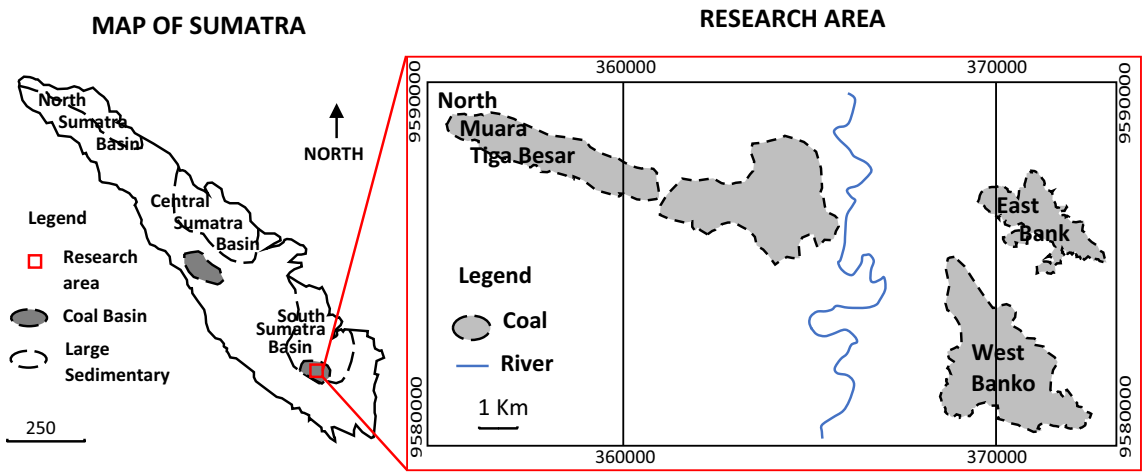


**Fig. 2** The location of the research area in South Sumatra Basin, Indonesia

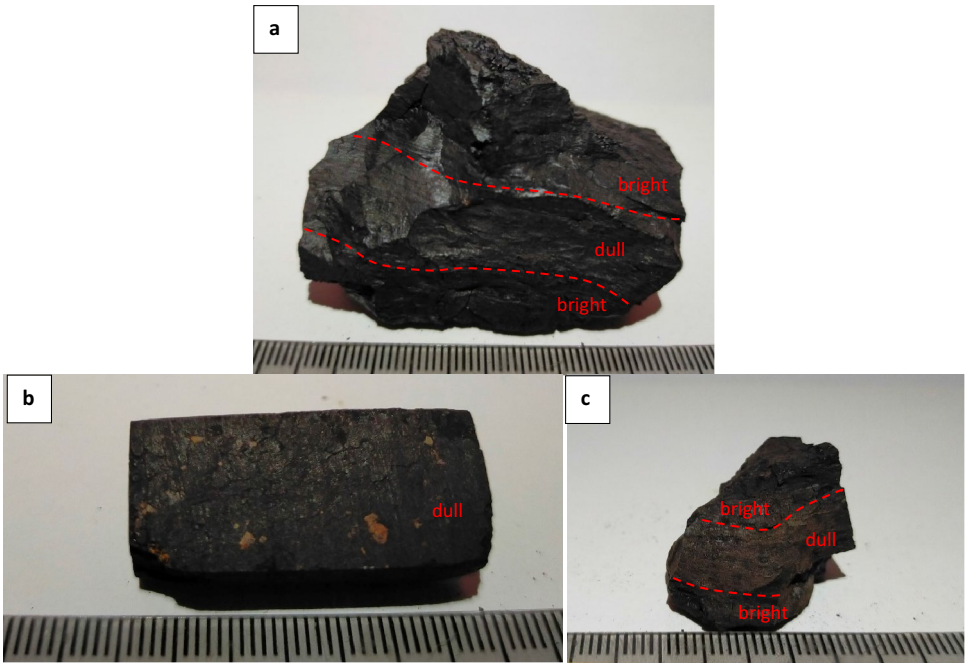


**Fig. 3** The lithotype of coal samples from **a** WB, **b** EB, and **c** NMTB

weighing approximately 1 g of coal, heating it to 105 ℃, and then re-weighing the dry sample at room temperature. Organic petrography was done by crushing the samples into 0.25 mm particles, mounting them in polyester resin, desiccating for 12 h, and polishing one of the flat surfaces. The polished coal sample was analyzed under a reflected light microscope to determine the maceral and huminite reflectance. Maceral analysis was conducted by counting 550 points per sample. Huminite reflectance was determined by analyzing 50 huminite grains as described in the ASTM D2798-06 guidelines. Huminite reflectance can also be defined by the volatile matter value where the equation follows (1) (Rice 1993).

$$R_0(\%) = -2.172 \times log\left(VM_{daf}\right) + 5.092 \quad (1)$$

## Adsorption measurements

The coal samples used for the adsorption analysis were coal powder crushed into 0.25 mm (60 mesh) particles and coal block (1 × 1 cm) created from the irregular-shaped coal, shaped and smoothed with sandpaper (Table 1). EB coal block sample was found to be slightly more brittle than the other coal block samples and have many cleats. The adsorption experiment used coal block and 5 g of coal powder

**Table 1** Coal sample from all coal fields in different coal forms

| Sample ID | Coal powder | Coal block |
|---|---|---|
| WB | 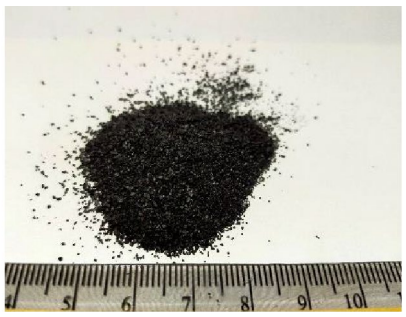 | 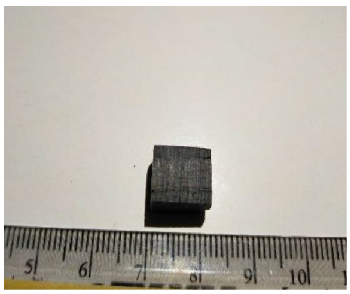 |
| EB |  |  |
| NMTB |  | 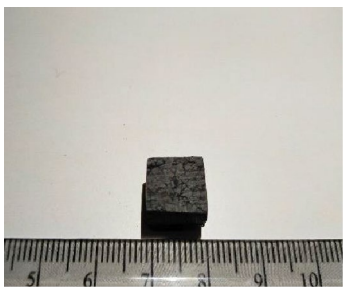 |

from all coalfields. For dry coals, coal samples were dried for 2–5 h in a vacuum oven at 105 ℃ until the weight of coal remained constant to remove the moisture content. The dried coal samples were transferred abruptly to the sample cell to avoid any exposure to oxidation or moisture after the drying process. The steps of the experimental process to identify $CO_2$ adsorption on coal are figured on the flowchart (Fig. 4).

## Experimental setups

The volumetric method was selected to determine coal adsorption. This study used different equipment to analyze coal powder and coal block. Conventional equipment analyzes $CO_2$ adsorption on coal powder since this equipment only allows a small volume. Newly manufactured equipment to hold large volumes use for analyzing $CO_2$ adsorption on coal blocks. The coal block adsorption equipment has been curved on the bottom to allow the $CO_2$ adsorption on every side of the cube. For coal powder, the $V_{rc}$ was 40 $cm^3$ and $V_{sc}$ was 75 $cm^3$ (Fig. 5 a). The $V_{rc}$ and $V_{sc}$ were the same for the coal block, 201 $cm^3$ (Fig. 5 b). The entire setup was placed in a water bath at a constant temperature (318.15 K). The $V_{void}$ was determined by subtracting the volume of sample from the volume of empty sample cell (Busch et al. 2003a). The sample volume was determined by dividing the mass of coal over the coal density. Adsorption analysis was conducted under six pressure steps (0.5, 1.0, 1.5, 2.0, 2.5, and 3.0 MPa) at 318.15 K. To reflect the in situ condition, the highest pressure in this experiment was adjusted at 3 MPa as the target was encountered at a shallow depth (Sosrowidjojo 2013). Higher pressure would not be suitable for reservoir conditions. $CO_2$ was subsequently introduced into the reference cell and allowed to equilibrate until no changes in the pressure were observed for 30 min. Finally, the reference cell was opened, and the system was allowed to equilibrate until there was no change in the pressure for 24 h.

Gibbs's excess adsorption equations were used in this study to calculate the amount of adsorbed gas on the

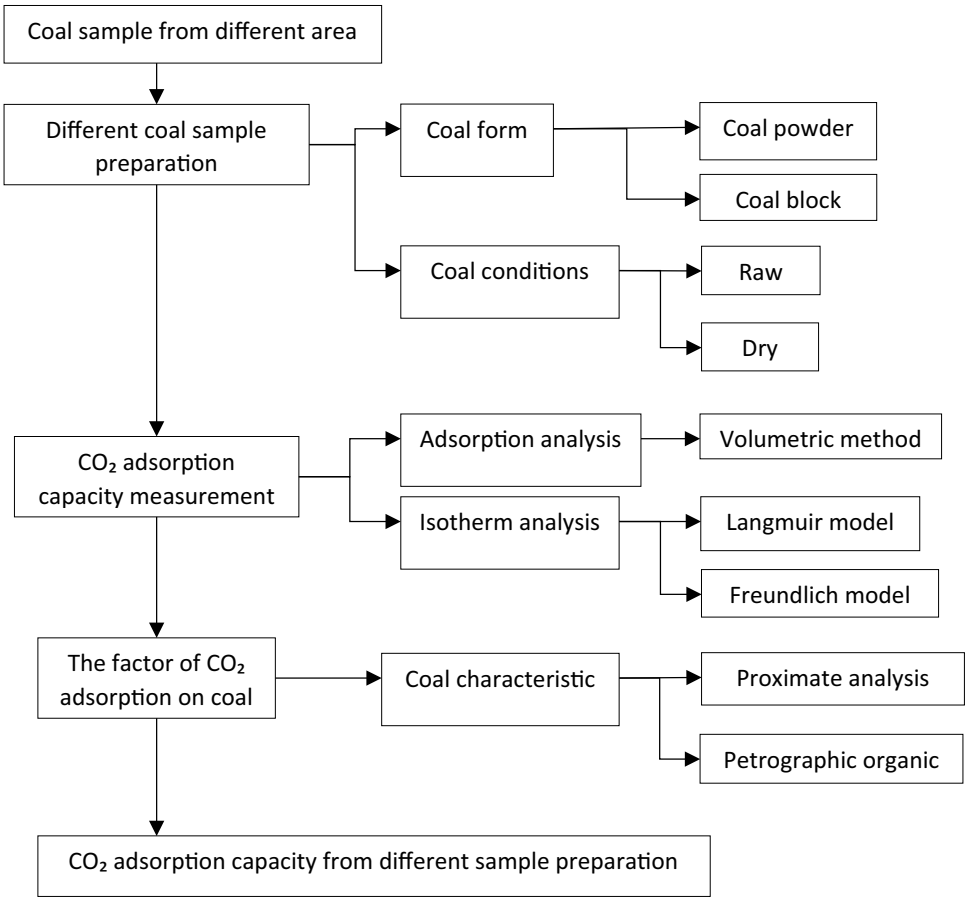


**Fig. 4** Flowchart of experimental process in this study

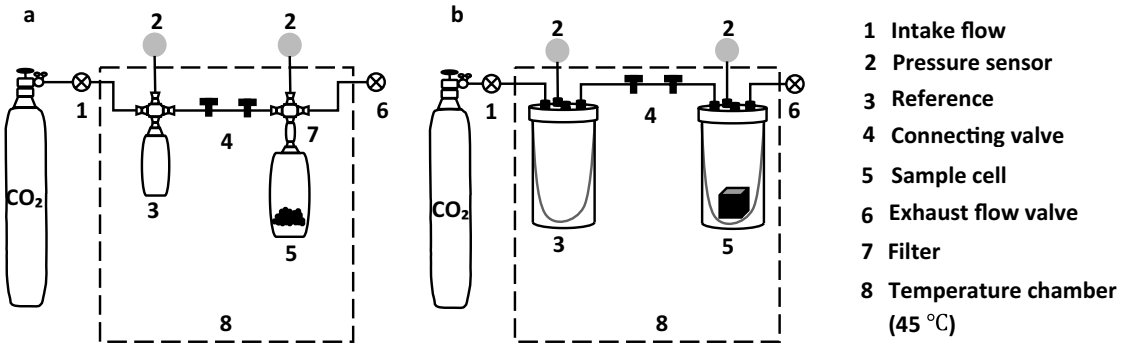


**Fig. 5** Volumetric method for **a** coal powder and **b** coal block

samples described as follows Eq. (2) (Goodman et al. 2004).

$$\Delta n^{ex} = \left(\frac{1}{RTm}\right)\left(V_{rc}\left(\frac{P_{rci}}{Z_{rci}} - \frac{P_{rcf}}{Z_{rcf}}\right) - V_{void}\left(\frac{P_{scf}}{Z_{scf}} - \frac{P_{sci}}{Z_{sci}}\right)\right) \tag{2}$$

where the compressibility factor was calculated as follows Eq. (3) (Abunowara et al. 2020).

$$Z = 1 + \left(0.083 - \frac{0.422}{T_r^{1.6}}\right)\frac{P_r}{T_r} + \omega\left(0.139 - \frac{0.172}{T_r^{4.2}}\right)\frac{P_r}{T_r} \tag{3}$$

where the reduced pressure were described in Eq. (4), and the reduced temperature were described in Eq. (5) (Abunowara et al. 2020).

$$P_r = \frac{P}{P_c} \tag{4}$$

**Table 2** Results of proximate analysis of coal samples

| Parameter | Sample | | |
|---|---|---|---|
| | *WB* | *EB* | NMTB |
| Moisture (%, ar) | 16.67 | 22.68 | 23.40 |
| ash (%, adb) | 2.12 | 1.09 | 1.76 |
| VM (%, adb) | 49.58 | 49.46 | 49.39 |
| FC (%, adb) | 50.42 | 50.54 | 50.61 |
| Huminite (%) | 64.43 | 58.92 | 52.00 |
| Liptinite (%) | 20.69 | 25.95 | 24.73 |
| Inertinite (%) | 13.43 | 12.07 | 21.27 |
| Mineral (%) | 1.45 | 3.06 | 2.00 |
| Ro (%) | 0.49 | 0.50 | 0.50 |

$$T_r = \frac{T}{T_c} \tag{5}$$

where the critical pressure of $CO_2$ is 7.39 MPa, the critical temperature of $CO_2$ is 304.2 K and the acentric factor of $CO_2$ is 0.224.

## Results and discussion

### Coal characteristic

The results of proximate and organic petrography analysis are shown in Table 2. The moisture content of samples from three different area varied, but the fixed carbon and volatile matter values were comparable (Fig. 6 a). Moisture has more substantial changes than fixed carbon and volatile matter compared to the lowest value of moisture content, fixed carbon, and volatile matter (Fig. 6b). A sample from West Banko (WB) showed lower moisture content (16%, a.r) than coal from East Banko (EB) (22%, a.r) and North Muara Tiga Besar (NMTB) (23%, a.r). Organic petrography showed huminite in WB coal sample is 64.43%, EB coal sample is 58.92% and NTMB coal sample is 52%. Liptinite was moderately present (20–25%) but inertinite occur with low concentrate (12–21%). Compared to other samples with the lowest particular maceral content, WB contain the highest huminite, EB contain the highest liptinite and NTMB contain the highest inertinite (Fig. 7). The WB coal sample had low ash yield and mineral due to the coal deposition, and no significant marine influence has been observed in this research area (Amijaya and Littke 2005). Ash yields are generally less than 5% correlating reasonably well with the mineral determined microscopically. Even though the moisture and organic content showed different values, the huminite reflectance was similar (0.49–0.50%). Based on the reflectance huminite classification (Thomas 2013), these coal samples are low-rank coal and classified as high volatile bituminous C.

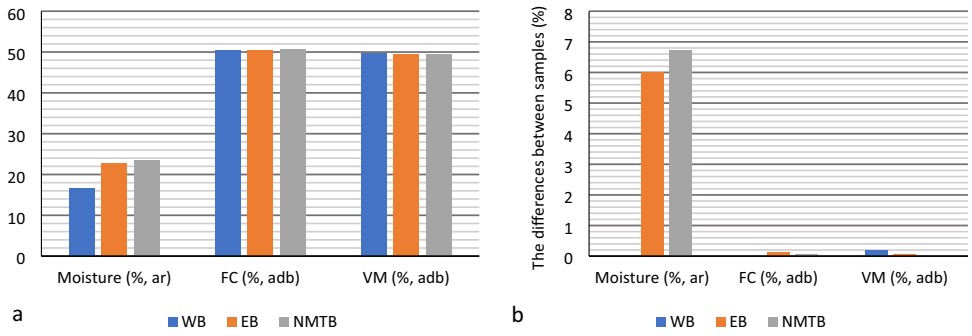


**Fig. 6** **a** The result of proximate analysis and **b** the differences coal samples with samples contained the lowest value of moisture, fixed carbon and volatile matter

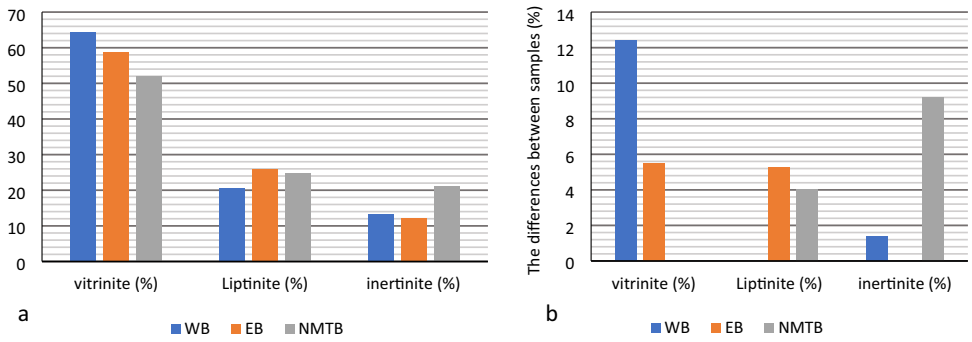


**Fig. 7** **a** The result of organic petrography and **b** the differences coal samples with samples contained the lowest value of huminite, liptinite and inertinite

## $CO_2$ adsorption measurement

$CO_2$ adsorption was analyzed over two parameters such as coal forms and moisture content. The different parameters showed the different times to reach equilibrium. The raw coal block samples took the longest, whereas dry coal powder took the shortest time to reach equilibrium. On average, the adsorption test on raw coal powder required 12 h to reach equilibrium in every pressure step; meanwhile, the dry condition only required 6–10 h. Experimental data for the raw coal block showed that it required 24–30 h to reach equilibrium in every pressure step. Meanwhile, the dry condition of the coal block needs 14–16 h in every pressure step.

For each parameter, such as coal form and moisture content, the result demonstrated a similar amount of $CO_2$ adsorption (Fig. 8). The highest amount of $CO_2$ adsorption was found on coal in powdered and dry conditions, while the lowest amount in coal samples with block and raw conditions. The difference in adsorption with different parameters gets higher along with higher pressure. The difference in moisture content is more significant than coal form, mainly found on lower pressure (0–1 MPa) when in raw coal, it is tough to find the difference; meanwhile, on dry coal, even in lower pressure, the difference is noticeable. Based on these findings, the method of preparing samples for $CO_2$ adsorption capacity measurement is an essential value. The $CO_2$ adsorption capacity of the coal study area was also compared with similar coal ranks from different coalfields worldwide (Table 3). By the comparison with another sample, this research found a similar trend, such as dry condition has bigger capacity than coal with moisture content, and compact coal sample has a lower capacity than powder coal. The comparison shows this study has a lower value than other research because this research uses lower pressure due to consider not only $CO_2$ storage but also ECBM. There is some uniformity in the outcomes across all condition, but there is still a minor variance. Coal characteristics play a critical role in the results despite crushing and drying. WB and EB coal samples had the highest and lowest $CO_2$ adsorption capability under all condition.

## Isotherm analysis

This study chose the Langmuir and Freundlich isotherm model to fit the experimental data. The Langmuir adsorption model defines the relationship between gas concentration and pressure for any coal on monolayer adsorption capacity.

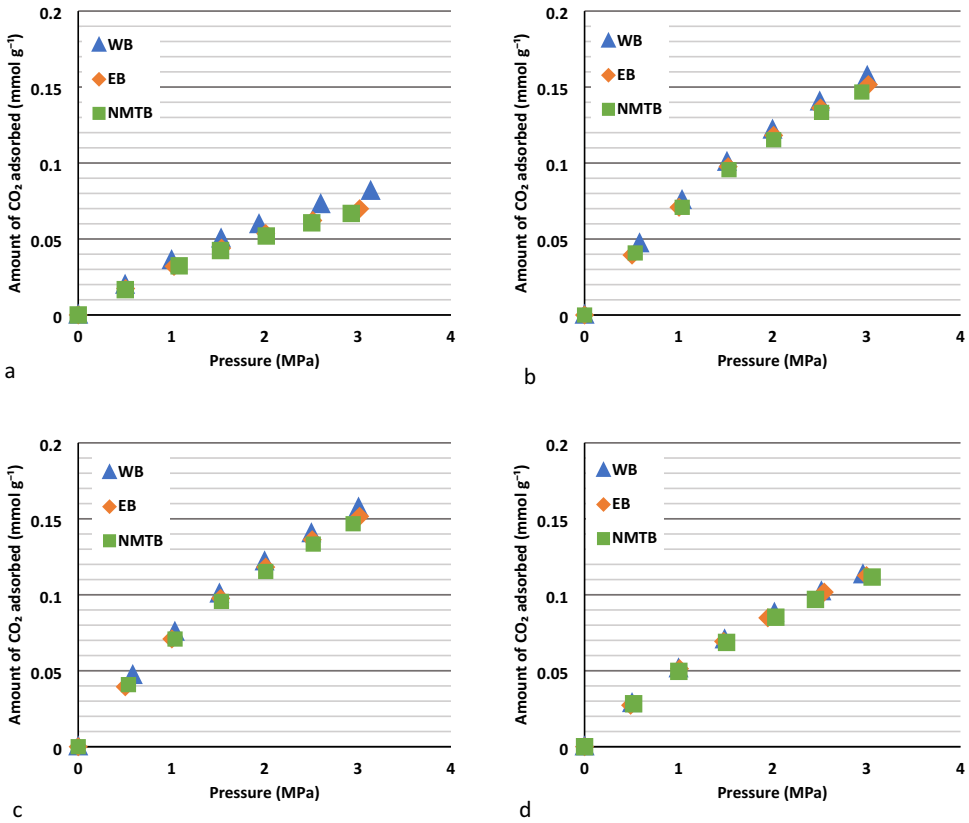


**Fig. 8** $CO_2$ adsorption on the difference between coal form and moisture: **a** powder samples under raw conditions, **b** powder samples under dry condition, **c** block samples under raw conditions, and **d** block samples under dry conditions

**Table 3** Summary of the $CO_2$ adsorption on low rank under various conditions

| Coal sample | Coal form | Experimental temperature | Experimental pressure | Wet $CO_2$ adsorption capacity (mmol $g^{-1}$) | Dry $CO_2$ adsorption capacity (mmol $g^{-1}$) | References |
|---|---|---|---|---|---|---|
| Bituminous Czech Republic coal samples | Coal powder (2 mm) | 318 K and 328 K | 0.1–0.8 MPa | 0.98 | 1.2 | (Weniger et al. 2012) |
| High to low volatile bituminous Czech Republic coal samples | Coal powder (0.2 mm) | 318 K | 20 MPa | 0.75 | 1.29 | (Švábová et al. 2012) |
| Subbituminous US coal samples | Coal powder (150–500 μ m) | 328 K | 12 MPa | 0.68 | 0.95 | (Romanov et al. 2013) |
| Subbituminous Malaysian coal samples | Coal powder (2.5–5 cm) | 348 K | 6 MPa | 0.2 | 0.7 | (Abunowara et al. 2020) |
| Subbituminous China coal samples | Coal core | 323.15 K | 16 MPa | | 0.3 | (Zhang et al. 2018) |
| High volatile bituminous Indonesian coal samples | Coal powder (0.25 mm) | 318.15 K | 3 MPa | 0.082 | 0.17 | This study |
| | Coal block (1 × 1 cm) | 318.15 K | 3 MPa | 0.065 | 0.12 | |

$G_a$ detailed calculation as follows Eq. (6) (Tiab and Donaldson 2016).

$$G_a = V_L\left(\frac{P}{P + P_L}\right) \tag{6}$$

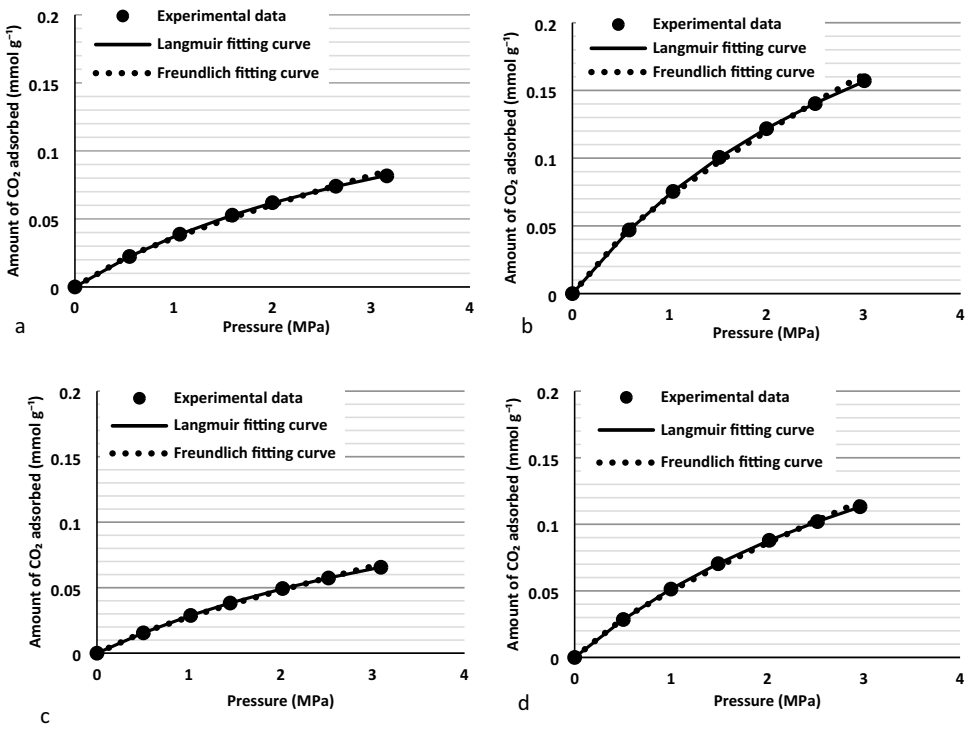


**Fig. 9** Comparison of different $CO_2$ adsorption experiment and isotherm fitting curve from WB coal samples with various conditions: **a** powder samples under raw condition, **b** powder samples under dry condition, **c** block samples under raw condition, and **d** block samples under dry condition

**Table 4** Constant $CO_2$ adsorption isotherm model

| Coal conditions | | Langmuir isotherm model | | | Freundlich isotherm model | | |
|---|---|---|---|---|---|---|---|
| | | *VL* | *PL* | $R^2$ | *n* | *k* | $R^2$ |
| Powder | Raw | 0.188 | 4.0843 | 0.999602 | 0.7461 | 0.036084 | 0.999017 |
| | Dry | 0.3604 | 3.9124 | 0.999727 | 0.7379 | 0.071855 | 0.999285 |
| Block | Raw | 0.1776 | 5.2708 | 0.998166 | 0.7979 | 0.027637 | 0.998376 |
| | Dry | 0.2908 | 4.6574 | 0.996016 | 0.7809 | 0.050047 | 0.998796 |

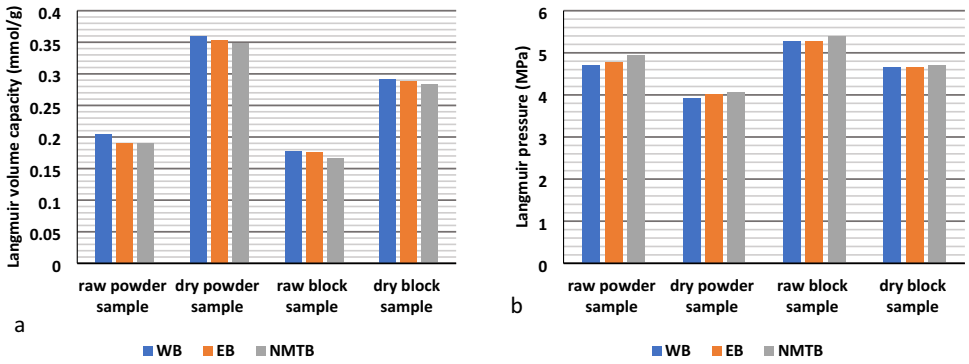


**Fig. 10** Langmuir parameters for $CO_2$ adsorption of all measured samples: **a** Langmuir volume capacity and **b** Langmuir pressure

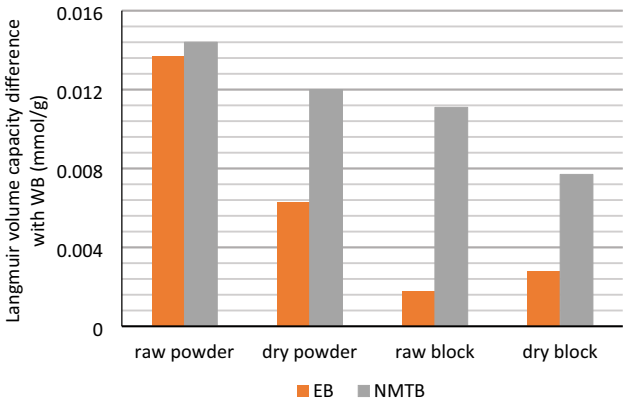


**Fig. 11** The difference in Langmuir volume capacity on EB and NMTB from WB coal sample

The Freundlich model is described the heterogeneity of coal surface by occurrence different adsorption energies on multilayers formation (Mahmoud et al. 2019). $Q_e$ calculated with detailed as follows Eq. (7) (Guarín Romero et al. 2018).

$$Q_e = K_f PCO_2^{\frac{1}{n}} \tag{7}$$

The least-squares method in the Excel solver function was applied to estimate the Langmuir and Freundlich isotherm models from the experimental data and draw the fitted line (Fig. 9). The correlation ($R^2$) from experimental and model show the fitting of the Langmuir as well as Freundlich isotherm model (Table 4), indicating monolayer as well as multilayer adsorption of $CO_2$ was observed.

## Langmuir parameter on $CO_2$ adsorption on coal

The Langmuir volume capacity shows similar results under all conditions, but the difference is discernible. WB coal sample found as the highest, and NTMB was found to have the lowest Langmuir volume capacity of all conditions (Fig. 10). Comparison of other samples on raw and dry conditions with WB coal sample showed moisture content had a significant effect (Fig. 11). The difference on raw condition easier to define than dry condition, expect on raw block coal samples. This condition related to the EB coal sample in the block form has a more visible cleat where gas is more accessible to adsorption into the coal sample. Langmuir pressure showed that the increasing water content and coal forms lead to the increase of Langmuir pressure. Previous studies have reported that $P_L$ was reciprocal to $V_L$, especially on the low-rank coal (Gensterblum et al. 2013). $P_L$ in the raw and block condition was higher than the dry and powder. As a result, $CO_2$ is more quickly absorbed in dry and powder conditions than in raw and block ones.

## Effect of different conditions on $CO_2$ adsorption capacity on coal

According to the preceding discussion, the crushing and drying processes increase $CO_2$ adsorption in coal. Comparing the discrepancy in Langmuir volume is due to various coal condition shows drying process resulted higher differences than crushing process (Fig. 12). Pervious research has shown

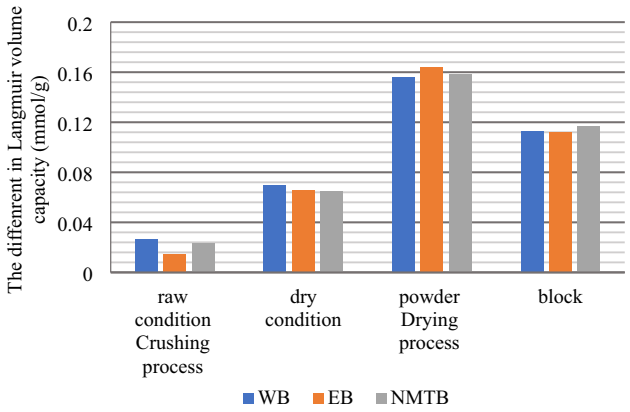


**Fig. 12** The discrepancy in Langmuir volume due to various coal conditions

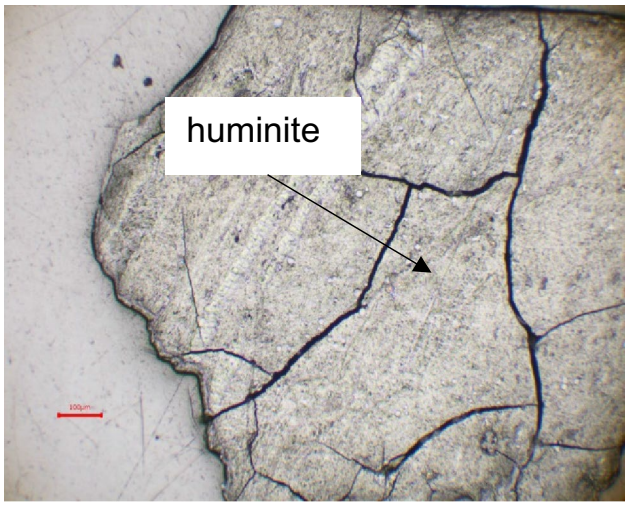


**Fig. 13** Huminite on coal sample on image under white light

that crushing coal causes the pore network to become more open (Olajossy 2017), which increases the surface area and produces more available sites to adsorb more gas, so the gas adsorption capacity is more significant in coal powder. However, coal powder and coal block showed similar adsorption capacity in raw conditions. The similarity shows that although changes in the surface area exist, the pore size distribution is still the same (Qi et al. 2017), so the changes are insignificant. A un-grind with a connected pore network provides more adsorption capacity than a grinded sample due to possibly increasing, decreasing, and even blockage pore (Mangi et al. 2022).

Experimental $CO_2$ adsorption capacity on low-rank coal resulted in the drying process having a significant effect. Low-rank coal contains much water because the absence of water in the pores causes significant changes in the coal (Yu et al. 2013; Olajossy 2017). Eliminating water content leads to losing water film on the pore wall surface and pore space (Zhao et al. 2018) and increasing micropore volume, which expands $CO_2$ adsorption capacity (Yu et al. 2013). The drying process resulted in excessive hydroxyl and carboxyl function groups, which intensified the possibility of $CO_2$ binding with active sites in coal (Abunowara et al. 2020).

## Effect of coal characteristics on $CO_2$ adsorption capacity of coal

This study uses correlation analysis (Dutta et al. 2011) to find the significant effect of the coal characteristics on $CO_2$ adsorption on coal. Based on the proximate analysis, in raw condition the moisture effect shows more significant differences than fixed carbon and volatile matter (Fig. 6). The elimination of moisture content by the drying process resulted in fixed carbon, and volatile matter affects more on $CO_2$ adsorption capacity (Fig. 11). Increasing fixed carbon is related to increasing $CO_2$ adsorption capacity (Dutta et al. 2011) and this also happened at WB coal sample with the highest fixed carbon resulted in the highest $CO_2$ adsorption capacity at raw and dry condition. The $CO_2$ adsorption capacity increased with decreasing volatile matter (Ramasamy et al. 2014), and these phenomena resulted in the similarity of $CO_2$ adsorption capacity in dry conditions due to EB and NTMB containing lower volatile matter than WB.

Organic matter content was essential for gas adsorption on coal (Mastalerz et al. 2004). Earlier research discovered huminite has considerable influence on $CO_2$ adsorbs on coal (Crosdale et al. 1998) due to the organic matter has associated micropore connections (Mangi et al. 2022). A similar result was also shown on coal in this experimental result. The experiment on $CO_2$ adsorption on coal samples shows a significant correlation between the role of huminite and $CO_2$ adsorption on coal (Fig. 7). The highest huminite content was found in the WB coal sample with the highest coal adsorption capacity (Fig. 13). Huminite can adsorb $CO_2$ effectivity due to its more micropore presence than other maceral content (Bakshi et al. 2020). WB coal sample contains the lowest liptinite compared with EB and NMTB but does not give significant results due to liptinite only weak positive correlation with pore network (Teng et al. 2017). In contrast to huminite and liptinite, inertinite inhibits adsorption processes (Mangi et al. 2020). The experimental result shows that NTMB contains the highest inertinite related with the lowest $CO_2$ adsorption capacity. Minerals also can reduce gas adsorption capacity due to infilling and blockage

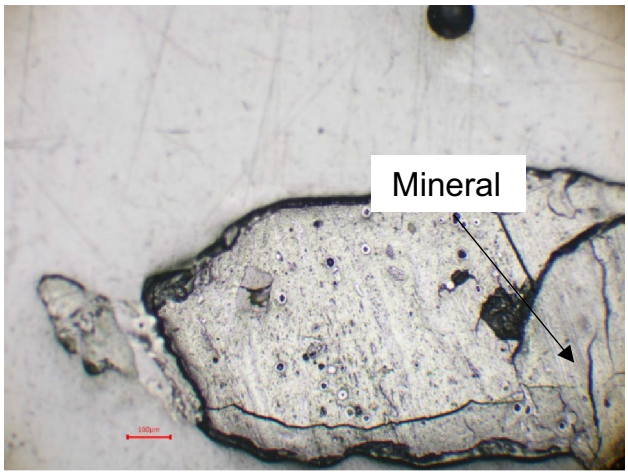


**Fig. 14** Mineral on coal sample under white light

of pores, cleats, fracture systems, and lower micropore surface area with inherent and extraneous minerals (Kumar et al. 2019; Mangi et al. 2020). By organic petrography analysis, the coal sample contains a mineral that possibly blocks coal pores and fractures (Fig. 14).

## Summary and conclusions

The following can be concluded as different coal preparation methods to measure $CO_2$ adsorption of seam B in different areas in the South Sumatera Basin, Indonesia, resulting in $CO_2$ adsorption capacity.

- Coal samples exhibited monolayer and multilayer adsorption of $CO_2$ at various conditions.
- $CO_2$ adsorption capacity in all condition shows similar results but have slight differences.$CO_2$ adsorption capacity in raw conditions was hard to find the significant difference between powder and block coal samples due to uncertainty on change pore network. The drying process allowed more accessible sites and increased $CO_2$ adsorption capacity. The drying process increases the effect on coal characteristics, even though the drying process might not depict a realistic situation.
- Coal sample from WB area more promising for $CO_2$ storage and ECBM due to lower moisture and higher huminite than EB and NMTB areas.

This study is an experimental laboratory approach to comparing adsorption capacity where the preparation such as drying and crushing processes clearly cannot represent the in situ condition. Moreover, it is implausible to be able to dry up low-rank coal to its full potential in natural situations.

**Acknowledgements** The authors thank PT Bukit Asam and the Unconventional Geo-Resources Research Group, Faculty of Engineering, Universitas Gadjah Mada, for providing the coal samples.

**Funding** No funding was received for this study.

## Declarations

**Conflict of Interest** The authors declare that they have no conflicts of interest.

**Ethical approval** The authors certify that this work is original, has not been published and will not be submitted elsewhere for publication.



## References

Abunowara M, Sufian S, Bustam MA et al (2020) Experimental measurements of carbon dioxide, methane and nitrogen high-pressure adsorption properties onto Malaysian coals under various conditions. Energy. https://doi.org/10.1016/j.energy.2020.118575

Afikah R, Sasaki K, Surjono SS, Amijaya DH (2018) The mechanical behaviour of coal relating to $CO_2$ sequestration of Tanjung Enim. Indonesia AIP Conf Proc. https://doi.org/10.1063/1.5066848

AlRassas AM, Ren S, Sun R et al (2021) CO2 storage capacity estimation under geological uncertainty using 3-D geological modeling of unconventional reservoir rocks in Shahejie Formation, block Nv32, China. J Pet Explor Prod 11:2327–2345. https://doi.org/10.1007/s13202-021-01192-4

Amijaya H, Littke R (2005) Microfacies and depositional environment of Tertiary Tanjung Enim low rank coal, South Sumatra Basin, Indonesia. Int J Coal Geol 61:197–221. https://doi.org/10.1016/j.coal.2004.07.004

Anggara F (2017) Site selection criteria for Geological $CO_2$ Sequestration : A Case Study from CO2-enhanced CBM recovery ( CO2 -ECBM ) in Indonesia. In: 6th World Conference on Applied Sciences, Engineering & Technology, 26–27, UMPO, Indonesia. pp 26–27

Anggara F, Sasaki K, Amijaya H, et al (2010) $CO_2$ Injection in Coal Seams, an Option for geological CO2 Storage and Enhanced Coal Bed Methane Recovery (ECBM). PROCEEDINGS, Indones Pet Assoc. https://doi.org/10.29118/ipa.1669.10.e.111

Anggara F, Sasaki K, Rodrigues S, Sugai Y (2014) The effect of megascopic texture on swelling of a low rank coal in supercritical carbon dioxide. Int J Coal Geol 125:45–56. https://doi.org/10.1016/j.coal.2014.02.004

Anggara F, Sasaki K, Sugai Y (2016) The correlation between coal swelling and permeability during CO2 sequestration: A case study using Kushiro low rank coals. Int J Coal Geol 166:62–70. https://doi.org/10.1016/j.coal.2016.08.020

Bakshi T, Vishal V, Prusty BK, Pathak K (2020) Carbon dioxide and methane sorption characteristics of Damodar Valley and Upper Assam shale. India Energy Clim Chang 1:100002. https://doi.org/10.1016/j.egycc.2020.100002

Battistutta E, Eftekhari AA, Bruining H, Wolf KH (2012) Manometric sorption measurements of $CO_2$ on moisture-equilibrated bituminous coal. Energy Fuels 26:746–752

Belkin HE, Tewalt SJ, Hower JC et al (2009) Geochemistry and petrology of selected coal samples from Sumatra, Kalimantan, Sulawesi, and Papua, Indonesia. Int J Coal Geol 77:260–268. https://doi.org/10.1016/j.coal.2008.08.001

Busch A, Gensterblum Y, Krooss BM (2003a) Methane and $CO_2$ sorption and desorption measurements on dry Argonne premium coals: pure components and mixtures. Int J Coal Geol 55:205–224. https://doi.org/10.1016/S0166-5162(03)00113-7

Busch A, Krooss BM, Gensterblum Y et al (2003b) High-pressure adsorption of methane, carbon dioxide and their mixtures on coals with a special focus on the preferential sorption behaviour. J Geochemical Explor 78–79:671–674. https://doi.org/10.1016/S0375-6742(03)00122-5

Chen MY, Cheng YP, Li HR et al (2018) Impact of inherent moisture on the methane adsorption characteristics of coals with various degrees of metamorphism. J Nat Gas Sci Eng 55:312–320. https://doi.org/10.1016/j.jngse.2018.05.018

Crosdale PJ, Beamish BB, Valix M (1998) Coalbed methane sorption related to coal composition. Int J Coal Geol 35:147–158. https://doi.org/10.1016/S0166-5162(97)00015-3

Day S, Fry R, Sakurovs R, Weir S (2010) Swelling of coals by supercritical gases and its relationship to sorption. Energy Fuels 24:2777–2783. https://doi.org/10.1021/ef901588h

De Silva PNK, Ranjith PG, Choi SK (2012) A study of methodologies for $CO_2$ storage capacity estimation of coal. Fuel 91:1–15. https://doi.org/10.1016/j.fuel.2011.07.010

Dutta P, Bhowmik S, Das S (2011) Methane and carbon dioxide sorption on a set of coals from India. Int J Coal Geol 85:289–299. https://doi.org/10.1016/j.coal.2010.12.004

Gao D, Hong L, Wang J, Zheng D (2019) Adsorption simulation of methane on coals with different metamorphic grades. AIP Adv. https://doi.org/10.1063/1.5115457

Gensterblum Y, Merkel A, Busch A, Krooss BM (2013) High-pressure $CH_4$ and $CO_2$ sorption isotherms as a function of coal maturity and the influence of moisture. Int J Coal Geol 118:45–57. https://doi.org/10.1016/j.coal.2013.07.024

Goodman AL, Busch A, Duffy GJ et al (2004) An inter-laboratory comparison of $CO_2$ isotherms measured on argonne premium coal samples. Energy Fuels 18:1175–1182. https://doi.org/10.1021/ef034104h

Guarín Romero J, Moreno-Piraján J, Giraldo Gutierrez L (2018) Kinetic and equilibrium study of the adsorption of $CO_2$ in ultramicropores of resorcinol-formaldehyde aerogels obtained in acidic and basic medium. C 4:52. https://doi.org/10.3390/c4040052

Hao D, Zhang L, Li M et al (2018) Experimental study of the moisture content influence on $CH_4$ adsorption and deformation characteristics of cylindrical bituminous coal core. Adsorpt Sci Technol 36:1512–1537. https://doi.org/10.1177/0263617418788444

Hao M, Qiao Z, Zhang H et al (2021) Thermodynamic analysis of $CH_4$/$CO_2$/$N_2$adsorption on anthracite coal: investigated by molecular simulation. Energy Fuels 35:4246–4257. https://doi.org/10.1021/acs.energyfuels.0c04337

Kalam S, Abu-Khamsin SA, Kamal MS, Patil S (2021) Surfactant adsorption isotherms: a review. ACS Omega 6:32342–32348. https://doi.org/10.1021/acsomega.1c04661

Karayiğit Aİ, Mastalerz M, Oskay RG, Buzkan İ (2018) Bituminous coal seams from underground mines in the Zonguldak Basin (NW Turkey): Insights from mineralogy, coal petrography, Rock-Eval pyrolysis, and meso-and microporosity. Int J Coal Geol 199:91–112. https://doi.org/10.1016/j.coal.2018.09.020

Khanal A, Shahriar MF (2022) Physics-based proxy modeling of $CO_2$ sequestration in deep saline aquifers. Energies 15:4350. https://doi.org/10.3390/en15124350

Kim D, Seo Y, Kim J et al (2019) Experimental and simulation studies on adsorption and diffusion characteristics of coalbed methane. Energies. https://doi.org/10.3390/en12183445

Kolak JJ, Burruss RC (2004) A Geochemical Investigation into the Effect of Coal Rank on the Potential Environmental Effects of CO2 Sequestration in Deep Coal Beds U . S . Department of the Interior

Kumar H, Mishra MK, Mishra S (2019) Sorption capacity of Indian coal and its variation with rank parameters. J Pet Explor Prod Technol 9:2175–2184. https://doi.org/10.1007/s13202-019-0621-1

Laxminarayana C, Crosdale PJ (1999) Role of coal type and rank on methane sorption characteristics of Bowen Basin, Australia coals. Int J Coal Geol 40:309–325. https://doi.org/10.1016/S0166-5162(99)00005-1

Liu Z, Zhang Z, Choi SK, Lu Y (2018) Surface properties and pore structure of anthracite, bituminous coal and lignite. Energies. https://doi.org/10.3390/en11061502

Mahmoud M, Eliebid M, Al-Yousef HY et al (2019) Impact of methane adsorption on tight rock permeability measurements using pulse-decay. Petroleum 5:382–387. https://doi.org/10.1016/j.petlm.2019.01.002

Mangi HN, Detian Y, Hameed N et al (2020) Pore structure characteristics and fractal dimension analysis of low rank coal in the Lower Indus Basin, SE Pakistan. J Nat Gas Sci Eng 77:103231. https://doi.org/10.1016/j.jngse.2020.103231

Mangi HN, Chi R, DeTian Y et al (2022) The ungrind and grinded effects on the pore geometry and adsorption mechanism of the coal particles. J Nat Gas Sci Eng 100:104463. https://doi.org/10.1016/j.jngse.2022.104463

Mastalerz M, Gluskoter H, Rupp J (2004) Carbon dioxide and methane sorption in high volatile bituminous coals from Indiana, USA. Int J Coal Geol 60:43–55. https://doi.org/10.1016/j.coal.2004.04.001

Masum SA, Chen M, Hosking LJ et al (2022) International journal of greenhouse gas control A numerical modelling study to support design of an in-situ $CO_2$ injection test facility using horizontal injection well in a shallow-depth coal seam. Int J Greenh Gas Control. https://doi.org/10.1016/j.ijggc.2022.103725

Olajossy A (2017) Some parameters of coal methane system that cause very slow release of methane from virgin coal beds (CBM). Int J Min Sci Technol 27:321–326. https://doi.org/10.1016/j.ijmst.2017.01.006

Pan Z, Connell LD, Camilleri M, Connelly L (2010) Effects of matrix moisture on gas diffusion and flow in coal. Fuel 89:3207–3217. https://doi.org/10.1016/j.fuel.2010.05.038

Qi L, Tang X, Wang Z, Peng X (2017) Pore characterization of different types of coal from coal and gas outburst disaster sites using low temperature nitrogen adsorption approach. Int J Min Sci Technol 27:371–377. https://doi.org/10.1016/j.ijmst.2017.01.005

Ramasamy S, Sripada PP, Khan MM et al (2014) Adsorption behavior of $CO_2$ in coal and coal char. Energy Fuels 28:5241–5251. https://doi.org/10.1021/ef500239b

Rice DD (1993) Composition and Origins of Coalbed Gas. In: Hydrocarbons from Coal. American Association of Petroleum Geologists, pp 159–184

Romanov VN, Hur TB, Fazio JJ et al (2013) Comparison of high-pressure CO2 sorption isotherms on Central Appalachian and San Juan Basin coals. Int J Coal Geol 118:89–94. https://doi.org/10.1016/j.coal.2013.05.006

Safaei-Farouji M, Vo Thanh H, Sheini Dashtgoli D et al (2022) Application of robust intelligent schemes for accurate modelling interfacial tension of $CO_2$ brine systems: implications for structural $CO_2$ trapping. Fuel 319:123821. https://doi.org/10.1016/j.fuel.2022.123821

Sosrowidjojo (2013) Coal Geochemistry of the Unconventional Muaraenim Coalbed Reservoir , South Sumatera Basin : a Case Study From the Rambutan Field. Indones Min J 71–81

Sripada P, Khan MM, Ramasamy S et al (2018) Influence of coal properties on the $CO_2$ adsorption capacity of coal gasification residues. Energy Sci Eng 6:321–335. https://doi.org/10.1002/ese3.201

Švábová M, Weishauptová Z, Přibyl O (2012) The effect of moisture on the sorption process of $CO_2$ on coal. Fuel 92:187–196. https://doi.org/10.1016/j.fuel.2011.08.030

Teng J, Mastalerz M, Hampton LB (2017) Maceral controls on porosity characteristics of lithotypes of Pennsylvanian high volatile bituminous coal: example from the Illinois Basin. Int J Coal Geol 172:80–94. https://doi.org/10.1016/j.coal.2017.02.001

Thomas L (2013) Coal Geology. John Wiley and Sons Ltd, West Sussex, UK

Tiab D, Donaldson EC (2016) Shale-Gas Reservoirs. Petrophysics. Elsevier, pp 719–774

Vo Thanh H, Sugai Y, Nguele R, Sasaki K (2019) Integrated workflow in 3D geological model construction for evaluation of $CO_2$ storage capacity of a fractured basement reservoir in Cuu Long Basin. Vietnam Int J Greenh Gas Control 90:102826. https://doi.org/10.1016/j.ijggc.2019.102826

Wahid A, Putra FA, Hidayat MT, Yusuf M (2018) Enhanced coal bed methane (ECBM) recovery optimization of CBM production using different injected gas composition and rate for south Sumatra CBM field Indonesia. E3S Web Conf 67:1–6. https://doi.org/10.1051/e3sconf/20186703015

Wang Q, Li W, Zhang D et al (2016) Influence of high-pressure $CO_2$ exposure on adsorption kinetics of methane and $CO_2$ on coals. J Nat Gas Sci Eng 34:811–822. https://doi.org/10.1016/j.jngse.2016.07.042

Wen H, Hao J, Ma L, Zheng X (2022) Experimental study on replacing coal seam $CH_4$ with $CO_2$ gas. ACS Omega 7:1395–1403. https://doi.org/10.1021/acsomega.1c06050

Weniger P, Franců J, Hemza P, Krooss BM (2012) Investigations on the methane and carbon dioxide sorption capacity of coals from the SW Upper Silesian Coal Basin, Czech Republic. Int J Coal Geol 93:23–39. https://doi.org/10.1016/j.coal.2012.01.009

Wu D, Liu G, Sun R, Chen S (2014) Influences of magmatic intrusion on the macromolecular and pore structures of coal: evidences from Raman spectroscopy and atomic force microscopy. Fuel 119:191–201. https://doi.org/10.1016/j.fuel.2013.11.012

Yu J, Tahmasebi A, Han Y et al (2013) A review on water in low rank coals: the existence, interaction with coal structure and effects on coal utilization. Fuel Process Technol 106:9–20. https://doi.org/10.1016/j.fuproc.2012.09.051

Zhang B, Liang W, Ranjith PG et al (2018) Effects of coal deformation on different-phase $CO_2$ permeability in sub-bituminous coal: an experimental investigation. Energies. https://doi.org/10.3390/en11112926

Zhao Y, Cao S, Li Y et al (2018) Experimental and numerical investigation on the effect of moisture on coal permeability. Nat Hazards 90:1201–1221. https://doi.org/10.1007/s11069-017-3095-9

Zhou Y, Li Z, Zhang R et al (2019) $CO_2$ injection in coal: advantages and influences of temperature and pressure. Fuel 236:493–500. https://doi.org/10.1016/j.fuel.2018.09.016

Zhu C, Wan J, Tokunaga TK et al (2019) Impact of $CO_2$ injection on wettability of coal at elevated pressure and temperature. Int J Greenh Gas Control 91:102840. https://doi.org/10.1016/j.ijggc.2019.102840